ChemComm

Accepted Manuscript

This article can be cited before page numbers have been issued, to do this please use: M. Bellare, V. K. Kadambar, P. Bollela, E. Katz and A. Melman, *Chem. Commun.*, 2019, DOI: 10.1039/C9CC03467F.

ROYAL SOCIETY OF CHEMISTRY

rsc.li/chemcomm

View Article Online
DOI: 10.1039/C9CC03467F

COMMUNICATION

Electrochemically Stimulated Molecule Release Associated with Interfacial pH Changes

Received 00th January 20xx,
Accepted 00th January 20xx

DOI: 10.1039/x0xx00000x

Madhura Bellare,† Vasantha Krishna Kadambar,† Paolo Bollella, Evgeny Katz,* Artem Melman*

A new linker with a hydrolyzable aryl ester bond was used for electrode modification. Basic pH locally produced at the electrode surface upon electrochemical reduction of O_2 resulted in the hydrolytic cleavage of the aryl ester bond and release of the immobilized fluorescent dye used as a model compound.

Signal-stimulated molecule release, being motivated by many biotechnological [1] and biomedical [2,3] applications, has been extensively studied over decades resulting in a large variety of physical and chemical systems operating differently and responding to different signals [4]. Among various molecule-releasing systems responding to different activating signals (optical [5], magnetic [6], chemical [7], mechanical [8], temperature change [9], etc.) electrochemical systems represent one of the most important and challenging research direction [10-13]. These systems might be relatively simple, being controlled by electrostatic attraction/repulsion of molecules at polarized electrode surfaces [14-16]. However, the approach based on electrostatically loaded/released molecules is not specific to any selected kind of molecules since different molecules having the same electrical charge respond to the electrical signals in the same way. More sophisticated systems being able to release only specific molecules are based on molecular and supramolecular systems, where the selected molecules are included in complex structures assembled at electrode surfaces and disassembled upon electrochemical processes [17-20]. Some of these systems have electrochemically cleavable covalent bonds [21,22] (e.g., disulfide bonds [23]), which can be broken by redox reactions resulting in the release of the connected molecules. While the electrochemical cleavage of bonds based on the redox transformations is a very powerful and successful approach in clean model systems, it may be significantly complicated in the presence of other redox species appearing in complex biological media. Thus, more universal approach to the electrochemically stimulated cleavage of chemical bonds should be investigated. This might be based on local pH changes accompanying oxygen reduction at an electrode surface, which can be easily achieved in all natural systems including various biochemical and biological media. Indeed, the electrochemical oxygen reduction resulting in formation of water or/and hydrogen peroxide consumes hydrogen ions and produces basic pH locally at the electrode surface, if the bulk solution is not a very strong buffer [16,24]. Chemical linkers cleavable at acidic pH values are available [25] and used in various biochemical applications. However, linkers hydrolysable at basic pH values produced locally at an electrode surface upon O_2 reduction are not common and have not been used for electrochemically triggered molecule release processes. Organic chemistry offers various groups sensitive to pH changes and hydrolysable at basic pH. One of the example is aryl esters, which are not stable at basic pH [26,27] and can be used for preparing linkers cleavable upon increasing local pH value at an electrode surface.

The present paper reports on the specially designed chemical linker containing aryl ester bond connecting molecules to an electrode and releasing them when the local pH increases due to electrochemical reduction of oxygen. The studied system provides a universal approach to the biomolecule release activated by electrochemical means without redox transformations of the linker and based exclusively on the hydrolytic process.

Department of Chemistry and Biomolecular Science, Clarkson University, Potsdam, NY 13699 (USA)
† These authors contributed equally to the work.
Electronic Supplementary Information (ESI) available: synthetic procedures, material characterization, electrode modification. See DOI: 10.1039/x0xx00000x

View Article Online
DOI: 10.1039/C9CC03467F

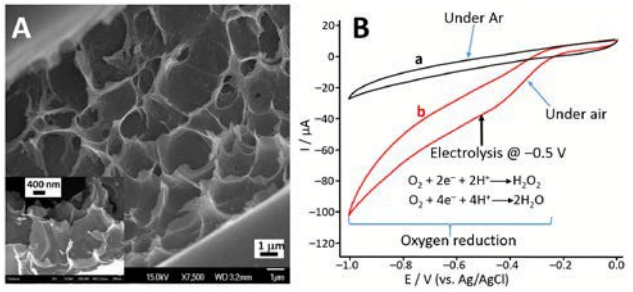

Fig. 1. (A) Scanning electron microscope (SEM) image of the graphene nanosheets produced on the carbon fibers. (B) Cyclic voltammograms recorded with the graphene modified electrode (25 mm^2 geometrical area) with the absence (a) and presence of O_2 (in equilibrium with air). Potential scan rate, 50 mV s^{-1}. Background electrolyte: phosphate buffer (3.0 mM, pH 7.2 containing 0.1 M NaCl).

Electrochemical oxygen reduction is one of the most studied processes proceeding at various electrodes based on different materials [28]. While different electrode materials can be used for preparing modified electrodes [29], graphene-based electrodes became recently very popular [30], particularly for bioelectrochemical applications [31]. The easiest way of preparing graphene-modified electrodes based on pilling graphene layers from carbon fibers upon their electrochemical treatment has been reported recently [32]. Figure 1A shows scanning electron microscope (SEM) image of the graphene nanosheets produced on the carbon fibers. The nanostructured surface provides high roughness and the unique electronic features of the graphene result in superior electrochemical properties of the modified electrode [32]. Oxygen reduction, specifically important for the present study, has been studied at graphene-based electrodes [33]. Figure 1B shows cyclic voltammograms obtained with the graphene-modified carbon fiber electrode in the absence and presence of O_2 (curves a and b, respectively). The electrochemical reduction of O_2 can proceed to the formation of H_2O_2 or H_2O, depending on the interface properties and potential applied [33]. Notably, both electrochemical processes proceeding at potentials more negative than –0.2 V (vs. Ag|AgCl|KCl, 3 M, reference electrode) result in consumption of hydrogen ions and local pH increase. The steady-state pH value in the vicinity to the electrode surface depends on the rates of two processes: consumption of hydrogen ions in the electrochemical O_2 reduction and diffusion of hydrogen ions from the bulk solution to the electrode surface according to the H^+ concentration gradient. In order to obtain significant pH change locally at the electrode surface, the current of the oxygen reduction should be large, meaning the fast reaction with the H^+ consumption. However, too negative potential may result in some side reactions, particularly if the process proceeds in complex biological media. The potential of –0.5 V was selected as the experimentally optimized value, which was enough to generate pH increase being enough to hydrolyze the aryl ester bond in the synthesized linker, but still not too much negative (note that in previously reported systems we applied –1.0 V potential for generating basic pH upon O_2 reduction [24]).

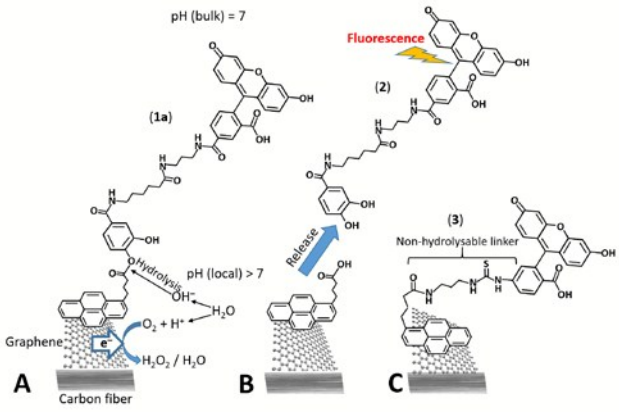

Fig. 2. (A) The structure of the linker with hydrolysable aryl ester bond and the fluorescent dye attached (only the 3-hydroxy isomer (**1a**) is shown; the second isomer (**1b**) is shown in the ESI). (B) The cleavage of the aryl ester bond at basic pH values and the release of fluorescent dye (**2**). (C) Fluorescein pyrene derivative (**3**) with a non-hydrolysable linker used in the control experiments.

Figure 2A shows schematically the structure of the linker and the fluorescent dye bound as a model compound (**1a**, the technical details on the synthetic procedures, material characterization and the electrode surface modification are collected in the Supporting Information). The linker was adsorbed on the graphene sheets due to non-covalent π-π stacking of pyrene groups to the graphene sheets [34]. This way to immobilize various biomolecules on aromatic electrode surfaces (including electrodes composed of carbon nanotubes [35] and graphene [36]) has been extensively used in different bioelectrochemical systems. When the potential of –0.5 V is applied in the presence of O_2 (in equilibrium with air), the local pH in a thin layer close to the electrode surface is increased, the aryl ester bond is hydrolyzed and the fluorescent dye (**2**) is released. The process was performed in 3 mM phosphate buffer, pH 7.2, with 0.1 M NaCl and the bulk pH value was not affected by the

electrochemical reaction. The electrochemically stimulated release was followed by measuring fluorescence in the bulk solution, Figure 2B and Figure 3, curve a. Prior to the potential application, the electrode was soaked in the background solution to characterize the uncontrolled leakage of the fluorescent dye from the electrode surface, Figure 3, curve a. The reasons for the minor fluorescence increase might be different, mostly related to the partial instability of the aryl ester bond, which could be hydrolized even at the neutral pH values, but with much smaller rate comparing to the basic pH values. The next experiment was aiming at estimation of the pH value locally produced at the electrode surface upon O_2 reduction. This was done by comparing the rate of the fluorescence increase in the solution upon electrochemical O_2 reduction and similar processes under different bulk pH values, Figure 4. As expected, the fluorescent dye release was stimulated by the bulk pH increase (see the red curves measured at the different bulk pH values). The electrochemically stimulated release proceeded with the rate similar to the process when the bulk pH was ca. 10.0–10.5. This result allows to estimate roughly the local pH generated by the O_2 reduction.

In order to confirm that the release process is indeed associated with the hydrolysis of the aryl ester bonds, we prepared another linker with all chemical bonds stable (non-hydrolyzable) at basic pH values, Figure 2C. The control experiments have shown some fluorescence increase in the solution when the potential of –0.5 V was applied (Figure 3, curve b) or the bulk pH was changed from pH 7.0 to pH 10.5 (Figure 3, curve c). However, the fluorescent dye release connected to the electrode via the non-hydrolyzable linker (**3**) was much smaller than in case of the hydrolyzable linker (compare curves b,c with a, Figure 3).

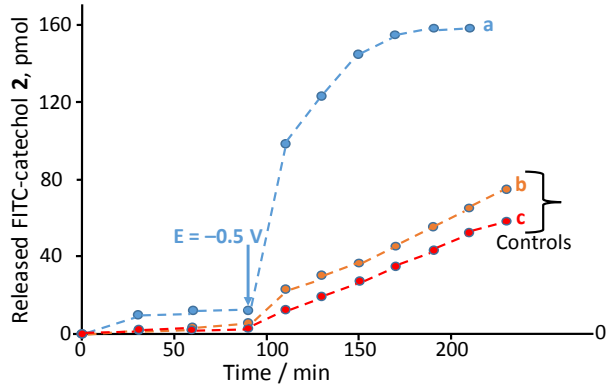

Fig. 3. Fluorescence measurements performed in the bulk solution upon leakage and signal-triggered release of the fluorescent dye: (a) the linker is hydrolysable and the cleavage of the aryl ester bond was achieved at the local basic pH generated electrochemically by O_2 reduction; (b) the linker is not hydrolysable and the release was obtained by polarization of the electrode at –0.5 V; (c) the linker is not hydrolysable and the release was obtained by applying bulk pH 10.5.

The minor release of the fluorescent dye bound to the electrode through non-hydrolyzable linker can be only explained by desorption of pyrene-anchor group from the electrode surface stimulated by either negative potential or basic pH value. It is known that the π-π stacking of pyrene groups at an aromatic electrode surface is a reversible process [37] and the pyrene groups can be removed from an electrode surface by different means [38]. The pyrene desorption from aromatic electrode surfaces can be affected by the applied potential and by pH value [39], exactly related to our control experiments with the non-hydrolyzable linker. Overall, the control experiments comparing the molecular release with the use of the hydrolyzable and non-hydrolysable linkers suggest that the major effect originates from the hydrolysis of the aryl ester bond, while minor contribution can result from the desorption of the pyrene-anchor group.

Conclusions

The present preliminary study demonstrated the powerful application of hydrolysable linkers for electrochemically stimulated

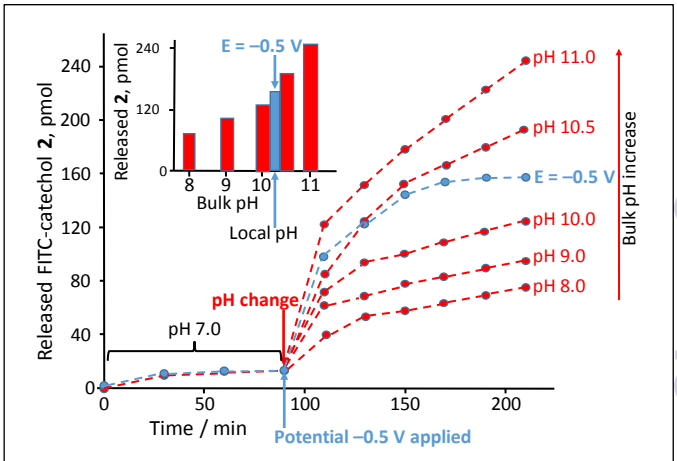

Fig. 4. Fluorescence measurements performed in the bulk solution upon leakage and signal-triggered release of the fluorescent dye triggered by applying different bulk pH values (the pH numbers are shown right to the red curves). The blue curve shows the release obtained by applying –0.5 V in the presence of O_2 (note that this curve is the same as shown in Figure 3, curve a). Inset: Comparison of the release kinetics measured with various bulk pH values and the electrochemically stimulated release.

local pH change. Based on the obtained results with the model fluorescent dye release, one can expect numerous systems where different biomolecular activators/inhibitors can be released to modulate biological processes, thus controlling biological processes by electronic means. While the biomolecular release in biological systems (including cellular systems) will require additional studies, particularly being complicated by high buffer capacitance of the biological media, some artificial systems can be straightforward. For example, activation of switchable enzymes [40] or biocomputing systems [41] can be easily integrated with the release systems based on the presented approach.

This work was supported in part by Human Frontier Science Program, project grant RGP0002/2018 to EK. The authors thank Prof. Kirill Alexandrov for stimulating discussions and support.

Conflicts of interest

There are no conflicts to declare.

Notes and references

1 B. Azeem, K. KuShaari, Z. B. Man, A. Basit, T. H. Thanh, *J. Control Release* 2014, **181**, 11–21.
2 *Fundamentals and Applications of Controlled Release Drug Delivery*, J. Siepmann, R. A. Siegel, M. J. Rathbone (Eds.), Springer, New York, **2012**.
3 Biorelated Polymers and Gels – Controlled Release and Applications in Biomedical Engineering, T. Okano (Ed.), Academic Press, Boston, **1998**.
4 *Controlled Release Systems: Advances in Nanobottles and Active Nanoparticles*, A. van Herk, J. Forcada, G. Pastorin (Eds.), CRC Press, Boca Raton, **2016**.
5 Z. Cao, Q. Lia, G. Wang, *Polym. Chem.* 2017, **8**, 6817–6823.
6 D. Mertz, O. Sandre, S. Bégin-Colin, *Biochim. Biophys. Acta, Gen. Subj.* 2017, **1861**, 1617–1641.
7 G. Kocak, C. Tuncer, V. Bütün, *Polymer Chem.* 2017, **8**, 144–176.
8 Y. Zhang, S. Sinha-Ray, A. L. Yarin, *J. Mater. Chem.* 2011, **21**, 8269–8281.
9 C. de la Torre, A. Agostini, L. Mondragón, M. Orzáez, F. Sancenón, R. Martínez-Máñez, M. D. Marcos, P Amorós, E. Pérez-Payáde, *Chem. Commun.* 2014, **50**, 3184–3186.
10 S. Szunerits, F. Teodorescu, R. Boukherroub, *Eur. Polym. J.* 2016, **83**, 467–477.
11 E. Honarvarfard, M. Gamella, N. Guz, E. Katz, *Electroanalysis* 2017, 29, 324–329.
12 R. Hang, J. Wu, C. Xi, N. Lehnert, T. Major, R.H. Bartlett, and M. E. Meyerhoff, *ACS Appl. Mater. Interfaces* 2014, **6**, 3779–83.
13 D. Correia-Ledo, A. A. Arnold and J. Mauzeroll*, J. Am. Chem. Soc*., 2010, **132**, 15120–15123.
14 J. Wang, M. Jiang, B. Mukherjee, *Bioelectrochemistry* 2000, **52**, 111–114.
15 J. Wang, G. Rivas, M. Jiang, X. Zhang, *Langmuir* 1999, **15**, 6541–6545.
16 E. Honarvarfard, M. Gamella, D. Channaveerappa, C. C. Darie, A. Poghossian, M. J. Schöning, E. Katz, *Electroanalysis* 2017, **29**, 1543–1553.
17 B. S. Aytar, M. R. Prausnitz, D. M. Lynn, *ACS Appl. Mater. Interfaces* 2012, **4**, 2726–2734.
18 F. Wang, D. Li, G. Li, X. Liu, S. Dong, *Biomacromolecules* 2008, **9**, 2645–2652.
19 F. Wang, J. Wang, Y. Zhai, G. Li, D. Li, S. Dong, *J. Control Release* 2008, **132**, 65–73.
20 F. Wang, X. Liu, G. Li, D. Li, S. Dong, *J. Mater. Chem.* 2009, **19**, 286–291.
21 W.-S. Yeo, M. N. Yousaf, M. Mrksich, *J. Am. Chem. Soc.* 2003, **125**, 14994–14995.
22 W.-S. Yeo, M. Mrksich, *Adv. Mater.* 2004, **16**, 1352–1356.
23 E. J. Moore, M. Curtin, J. Ionita, A. R. Maguire, G. Ceccone, P. Galvin, *Anal. Chem.* 2007, **79**, 2050–2057.
24 M. Masi, M. Gamella, N. Guz, E. Katz, *Electroanalysis* 2016, **28**, 2613–2625.
25 C. J. Choy, J. J. Geruntho, A. L. Davis, C. E. Berkman, *Bioconjugate Chem.* 2016, **27**, 824−830.
26 F. A. Carey, R. J. Sundberg, *Advanced Organic Chemistry: Part A: Structure and Mechanisms*, 5th ed., Springer, 2007, pp. 655–656.
27 M. Smith, March's Advanced Organic Chemistry: Reactions, Mechanisms, and Structure, 7th ed., Wiley, Hoboken, New Jersey, 2013, p. 1191.
28 M Shao, Q. Chang, J.-P. Dodelet, R. Chenitz, *Chem. Rev.* 2016, **116**, 3594−3657.
29 R. W. Murray, *Acc. Chem. Res.* 1980, **13**, 135–141.
30 X. Huang, Z. Y. Zeng, Z. X. Fan, J. Q. Liu, H. Zhang, *Adv. Mater.* 2012, **24**, 5979–6004.
31 P. Suvarnaphaet, S. Pechprasarn, *Sensors* 2017, **17**, art. No. 2161.
32 A. Koushanpour, N. Guz, M. Gamella, E. Katz*, Electroanalysis* 2016, **28**, 1943–1946.
33 D. Higgins, P. Zamani, A. Yu, Z. Chen, *Energy Environ. Sci.* 2016, **9**, 357–390.
34 M. Hinnemo, J. Zhao, P. Ahlberg, C. Hägglund, V. Djurberg, R. H. Scheicher, S.-L. Zhang, Z.-B. Zhang, *Langmuir* 2017, **33**, 3588–3593.
35 L. Halámková, J. Halámek, V. Bocharova, A. Szczupak, L. Alfonta, E. Katz, *J. Am. Chem. Soc.* 2012, **134**, 5040–5043.
36 A. Koushanpour, N. Guz, M. Gamella, E. Katz, *ECS Journal of Solid State Science and Technology* 2016, **5**, M3037-M3040.
37 N. Kong, J. J. Gooding, J. Liu, *J. Solid State Electrochem.* 2014, **18**, 3379–3386.
38 H. Ozawa, N. Katori, T. Kita, S. Oka, M. A. Haga, *Langmuir* 2017, **33**, 11901–11910.
39 M. M. Cao, A. P. Fu, Z. H. Wang, J. Q. Liu, N. Kong, X. D. Zong, H. H. Liu, J. J. Gooding, *J. Phys. Chem. C* 2014, **118**, 2650–2659.
40 M. Gamella, Z. Guo, K. Alexandrov, E. Katz, *ChemElectroChem* 2019, **6**, 638–645.
41 S. Mailloux, Y.V. Gerasimova, N. Guz, D.M. Kolpashchikov, E. Katz, *Angew. Chem. Int. Ed.* 2015, **54**, 6562-6566.